Efficient synergistic combination effect of Quercetin with Curcumin on breast cancer cell apoptosis through their loading into Apo ferritin cavity

(Article begins on next page)

07 January 2023

Efficient synergistic combination effect of Quercetin with Curcumin on breast cancer cell apoptosis through their loading into Apo ferritin cavity

Fariba Mansourizadeh [a,b#] , Diego Alberti [a#] , Valeria Bitonto [a] , Martina Tripepi [a] , Houri Sepehri [b] , Sepideh Khoee [c] , Simonetta Geninatti Crich [a*]

a. Department of Molecular Biotechnology and Health Sciences, University of Torino, via Nizza 52, 10126 Torino, Italy
b. Department of Animal Biology, School of Biology, College of Science, University of Tehran, Tehran, Iran.
c. Polymer Chemistry Department, School of Science, University of Tehran, PO Box 14155-6455, Tehran, Iran

[#] These authors contributed equally to this work

  * Corresponding author

e-mail: simonetta.geninatti@unito.it
tel: +39011 6706473
fax: +39 0116706487

Abstract

Combination of natural agents has received a great attention in cancer treatment because of synergistically increased apoptotic effect on cancer cell lines by triggering several apoptotic signaling pathways. However, the hydrophobic nature, poor bioavailability and low cellular uptake of most natural agents limit their therapeutic effectiveness. The purpose of this study was to design Apoferritin nanoparticles loaded with Quercetin and Curcumin (Que-Cur-HoS-Apo NPs) and to test their synergistic antitumor properties on a breast cancer cell line (MCF7). The physico-chemical characterization of the Que-Cur-HoS-Apo NPs by Size Exclusion Chromatography (FPLC) and Dynamic Light Scattering (DLS) confirmed the encapsulation of the compounds in the protein cage with narrow size distribution in the range 17.4±1.2 nm. Cell viability study indicated that Que-Cur-HoS-Apo NPs were able to exert a more pronounced effect at lower dose on the MCF7 cell line when compared to the free combination of the drugs. The Que-Cur-HoS-Apo system allowed cellular uptake of natural agents thus triggering enhanced apoptosis. These effects were confirmed by Annexin-V/7-AAD Staining Assay and intracellular Reactive Oxygen Species (ROS) quantitative detection. These results suggest the potential of Que-Cur-HoS-Apo NPs as a promising anti-cancer agent in breast cancer therapy and pave the way to examine Que-Cur-HoS-Apo NPs effect *in vivo*.

Keywords: Apoferritin, Quercetin, Curcumin, Breast Cancer, combined therapy

1. Introduction

Breast cancer is the most frequently diagnosed malignant tumor among women worldwide and is the primary cause of cancer death in women[1]. It is estimated that, approximately ca. 250,000 new cases of invasive breast cancer and more than 40,000 breast cancer deaths were diagnosed among US women in 2017[2].

Cancer is a multifaceted disease that is associated with a high degree of heterogeneity and adaptability[3]. At the present, there are three basic approaches for treating cancer: surgery, chemotherapy and radiotherapy. However, all of these methods have considerable side effects and often are not adequate for a successful treatment of metastasis[4]. For these reasons, taking into account cancer biology, there is a growing interest in the development of targeted drug delivery systems that can kill cancer cells with a simultaneous reduction of the toxicity for healthy tissues[4]. In this context, there is an increased attention in the use of herbal medicines and natural active compounds as promising agents for the cancer treatment. They show a great ability to inhibit fundamental processes for cancer cell proliferation with limited toxicity for healthy tissues and organs. Furthermore, nearly 80% of all drugs approved by FDA for cancer therapy during the last three decades are either natural products or are based thereon, or mimicked natural products[5, 6].

Flavonoids have recently received considerable attention as dietary supplements for cancer management. Quercetin (3, 3', 4', 5, 7-pentahydroxyflavone) is one of the most abundant flavonoid found in many vegetables and fruits that was reported to exhibit anti-oxidant, anti-inflammatory and anti-cancer effects through the inhibition of several intracellular signaling pathways[7, 8, 9]. Moreover, Quercetin has the second advantage of protecting healthy cells from chemotherapies induced cytotoxicity[10]. On the other hand, in tumor cells, Curcumin can inhibit cellular proliferation and angiogenesis, block cell cycle progression and induce apoptosis[11]. However, the generally poor solubility, bioavailability, stability and target specificity, together with the side-effects observed when used at high dose, have limited its use[12, 13].

Considering that cancer is a multi-step pathology, drugs combination, acting on multiple pathways, generates synergistic cancer cells death[14, 15]. There are different studies that investigated the mechanism of action of combined therapy with natural products. For example, it has been reported that Quercetin affects the expression and function of PGP (permeability glycoprotein) as ABC (ATP binding Cassette) efflux pump that may intensify action of cytotoxic drug and suppress the multi-drug resistance[10, 16]. Furthermore, some anti-tumor drugs such as doxorubicin and oxaliplatin induce different secondary effects which are associated with generation of ROS that are highly cytotoxic also for healthy cells[17].

Recent studies have found that the blockade of different signaling pathways observed with combinations of Quercetin and Curcumin might result in a more efficient anti-tumor effect, when compared with the single agent treatment[18].

To overcome the extremely low bioavailability and others limitations of these compounds, modern techniques such as structural modifications and various nano formulations were explored. Nanotechnology combination therapy, is an innovative approach that has potential applications in medical research[13]. Indeed, nanoparticles (NPs) can increase solubility and improve stability of phytochemicals, enhance their cellular absorption, protect them from immature degradation in the blood and increase their circulation time[19]. Various delivery platforms including liposomes, polymeric nanoparticles, polymeric micelles, dendrimers and micro emulsions are emerging as viable alternatives that have been shown to selectively deliver flavonoids at the tumor sites[13,19,20].

This study is focused on the use of Apoferritin nano cage as carrier for both Quercetin and Curcumin to perform a targeted cancer therapy. Apoferritin encapsulation has several advantages over the use of exogenous NPs, mainly due to its biocompatibility and biodegradability[21, 22]. Ferritins are a class of iron storage proteins that are widely distributed in most living organisms. Ferritin is composed of 24 subunits, including both heavy (H) chains (21 kDa) and light (L) chains (19 kDa). They self-assemble to form a spherical, shell-like structure that has inner and outer diameter of ~8 and ~12 nm, respectively[23]. In addition, thanks to its ability to disassemble and reassemble in a shape memory, Apoferritin has become an excellent platform for selective drug delivery. Apoferritin subunits may self-assemble into nanoscale cages with affinity towards Scavenger Receptor Class A member 5 (SCARA5) recognized by L chains and/or Transferrin Receptor 1 (TfR1) receptors recognized by H chains. Ferritin has also the potential to be conjugated with specific ligands or genetically modified protein to form chimeric fusion proteins or peptides on its surface[24, 25]. Finally, ferritin presents a unique architecture, surface properties, high biocompatibility and stability, homogenous narrow size (*ca.* 12 nm)[21, 23, 25, 26].

In the present work, the synergistic anti-tumor effect of Quercetin and Curcumin dissolved in the cell culture medium or co-delivered into the Horse Spleen Apoferritin (HoS-Apo) cavity, was evaluated to achieve an enhanced apoptotic effect on human breast cancer cell line MCF7. In fact, MCF7 overexpress SCARA5 receptors [27] that can be exploited for the selective delivery of HoS-Apo. The effect of the compounds on cell viability, apoptosis, ROS generation, as well as cell uptake was investigated. This is the first study that evaluates the therapeutic efficacy of two natural compounds encapsulated in Apoferritin cavity.

2. Materials and methods

2.1. Materials

Human breast cancer cell line (MCF7) and human breast epithelial cell line (MCF10A) were obtained from ATTC. EMEM and DMEM/F12 media, Fetal Bovine Serum (FBS), Horse serum, penicillin, streptomycin, L-glutamine, non-essential amino acid, sodium pyruvate were

obtained from Lonza. Apoferritin from equine spleen (HoS-Apo), Quercetin (Que), Curcumin (Cur) and all other chemicals used in this study were purchased from Sigma-Aldrich.

2.2. Nanoparticle preparation

In this study, three samples were prepared: HoS-Apoferritin loaded with Que (Que-HoS-Apo), HoS-Apoferritin loaded with Cur (Cur-HoS-Apo) and HoS-Apoferritin loaded with both Que and Cur (Que-Cur-HoS-Apo). The loading of compounds in the Apoferritin cavity was carried out following the already reported method[21]. Briefly, 250 µL of HoS-Apo were dissolved in 4.75 mL of distilled water and then the Apoferritin was dissociated into its subunits by lowering down the pH of the protein solution (4.1×10^{-6} mol/L) to 2 using HCl 1 M. The solution was maintained under stirring for 15 minutes. Afterwards, for Que-HoS-Apo and Cur-HoS-Apo preparation, 25 µL of Que and Cur solutions in DMSO (200 mg/mL) were added individually to the protein solution maintained at pH 2 and then stirred for 5 minutes. To prepare HoS-Apo loaded with both Que and Cur (Que-Cur-HoS-Apo), 25 µL of a Que solution in DMSO (200 mg/mL) and 25 µL of a Cur solution in DMSO (200 mg/mL) were added together to HoS-Apo solution maintained at pH 2 and the solution was stirred for 5 minutes. Consecutively, the pH was adjusted to 7.4 using 1 M NaOH for all the preparations. The resulting solutions were further stirred at room temperature for 2 h and then, they were transferred to a dialysis bag (14000 Da cut-off) and placed in a NaCl 0.15 M HEPES 3.8 mM buffer (pH 7.4) for 48 h, under stirring at 4°C. Then, the solutions were centrifuged for 10 minutes at 3000 rpm. After centrifugation, the supernatants were concentrated by using Sartorius Vivaspin centrifugal concentrators (50000 Da cut-off). At the end of this process the remaining amounts of the protein, Que and Cur were measured by Bradford assay and High Performance Liquid Chromatography (HPLC), respectively.

2.3. Nanoparticle characterization

2.3.1. HPLC assay for evaluation of Que-Hos-Apo, Cur-Hos-Apo, Que-Cur-HoS-Apo loading efficiency

The encapsulation of Curcumin, Quercetin and both the molecules was assessed using HPLC. Standard solutions of Curcumin and Quercetin dissolved in methanol were prepared and two calibrations curves were established. Calibration curve of Curcumin was performed at 430 nm whereas calibration curve of Quercetin was performed at 370 nm. The concentration of drugs in the samples were extrapolated from calibration curves based on the evaluation of the peak area of Curcumin and Quercetin.

The drug loading efficiency was determined by HPLC on a Waters Alliance-HPLC system equipped with 2695-Separation Module connected to 2998-Photodiode Array. A reverse-phase Waters XBridge C18, 150 mm × 4.6 mm ID, 5 µm at 25°C was used as the column. An isocratic elution mode was used with a mobile phase consisting of 0.1% phosphoric acid-acetonitrile (50:50 v/v). The effluent was monitored at 430 nm and 370 nm and the flow rate was 1.2 mL/min. The retention times (Tr) of Quercetin and Curcumin were found to be 2.26 min and 5.99 min, respectively.

Quercetin and Curcumin standard solutions (0.5 mg/mL), dissolved in methanol, were diluted to the range 2-50 µg/mL for standard calibration curves (R^2_{Que} = 0.9988, R^2_{Curc} = 0.9977).

Aliquots of 400 µL of Que-HoS-Apo, Cur-HoS-Apo and Que-Cur-HoS-Apo samples were brought to pH 2, sonicated in an ultrasonic bath in 1.2 mL of ethanol for 30 min. After centrifugation at 6000 rpm for 20 min and evaporation of the solvent, they were freeze-dried and resuspended in 400 µL of elution buffer. The samples underwent to another cycle of centrifugation to eliminate residues of protein and then they were analyzed by HPLC injecting 20 µL of sample. The encapsulation efficiency of the different samples was defined by the molar ratio between the encapsulated measured drugs and the protein Apoferritin.

2.3.2. Fast Protein Liquid Chromatography (FPLC)

The encapsulation of Quercetin and Curcumin in the Apoferritin cavity was confirmed by Size Exclusion Chromatography (SEC) performed on a FPLC system (ÄKTA purifier, GE Healthcare) equipped with a triple wavelength UV detector and an appropriate column (Superose 6, GE Healthcare). A volume of 100 µL of a 1 mg/mL protein solution was injected and 0.15 M NaCl 3.8mM HEPES buffer prepared with MilliQ purified water was used as eluent with a flow rate of 0.5 mL/min.

To verify the success of the encapsulation process, the three different curves recorded at the maximum UV-Vis absorption wavelengths of the HoS-Apo protein (280 nm), Quercetin (370 nm) and Curcumin (430 nm) were compared.

In order to evaluate the amount of Quercetin and Curcumin that remain non-specifically bound to the external protein surface, a second experiment was performed by incubating the Apoferritin in the presence of the same concentration of Quercetin and Curcumin at room temperature and pH 7.4 for 2 h without performing any dissociation/reassociation procedure.

2.3.3. Nanoparticle size analysis

The mean diameter of nanoparticles was measured by Dynamic Light Scattering (DLS) performed on Malvern Zetasizer 3000HS (Malvern, U.K.). All samples were analyzed at temperature T = 25 °C in filtered (cut-off, 200 nm) 0.15M NaCl 3.8mM HEPES buffer (pH 7.4). The mean diameter was obtained by the number-weighted distributions that represent the number of molecules in each bin in a given histogram, derived from the intensity distribution using the Mie theory. The particle size distribution is derived from a deconvolution of the measured intensity autocorrelation function of the sample using a non-negatively constrained least-squares (NNLS) fitting algorithm, a common example being CONTIN.

2.3.4. *In vitro* Que and Cur release

Que-Hos-Apo, Cur-HoS-Apo and Que-Cur-Hos-Apo in 0.15 M NaCl 3.8 mM Hepes buffer (2mL at a HoS-Apo concentration of 4µM) were transferred to dialysis bags (14000 Da cut-off) and placed in 40 mL of NaCl HEPES buffer at 37°C. The buffer was refreshed after 6, 24 and 48h. At these time, 400 µL of Que-Hos-Apo, Cur-HoS-Apo and Que-Cur-Hos-Apo were taken, brought to pH 2 and sonicated in an ultrasonic bath in 1.2 mL ethanol for 30 min. After centrifugation at 6000 rpm for 20 min and evaporation of the solvent, they were freeze-dried, resuspended in 400 µL of elution buffer and then analyzed by HPLC, as described above. The

recovery of Que and Cur was calculated as percentage difference measured at the various time intervals (6, 24 and 48h) with respect to t=0 set to 100%.

2.4 Cell Culture

The human breast cancer cell line MCF7 was cultured in EMEM medium containing 10% (v/v) FBS, 100 U/mL penicillin and streptomycin, 1% (v/v) non-essential amino acid, 1 mM sodium pyruvate, 2 mM L-glutamine and 0.01 mg/mL insulin. MCF10A cell line is a non-tumorigenic epithelial cell line and was cultured in DMEM/F12 medium containing 5% (v/v) Horse Serum, 100 U/mL penicillin and streptomycin, 100 ng/mL Cholera Toxin, 20 ng/mL Epidermal Growth Factor (EGF), 2 mM L-glutamine, 500 ng/mL hydrocortisone and 0.01 mg/mL insulin. MCF7 and MCF10A cells were maintained in a 5% CO_2 incubator at 37°C.

2.5 Cell cytotoxicity evaluation

The cytotoxicity of Cur, Que, Cur-HoS-Apo, Que-HoS-Apo and the synergic effects of Cur + Que or Que-Cur-HoS-Apo compounds on MCF7 and MCF10A were evaluated by MTT assay. Firstly, stock solution of Cur (200 mM) and Que (200 mM) were prepared in DMSO. The final DMSO concentration used in the assays was always kept below 0.2% (v/v). MCF7 and MCF10A cells were seeded into 96-well plates (4000 cells/well), respectively, in 100 µL of medium and allowed to attach for 24 h before treatment. The cells were exposed to various doses of Que and Cur and Que + Cur in the range of 0-100 µM for 48 h and HoS-Apo in the range 0-1µM. In the Que + Cur condition, the concentration incubated in the presence of cells was the sum of Que + Cur concentration and the molar ratio between Que and Cur was 1.1 as in HoS-Apo NPs. After the incubation, the medium was removed and replaced with 100µL of 0.45 mg/mL of a Thiazolyl Blue Tetrazolium Bromide dissolved in medium to each well and incubated for other 4 h at 37°C. Then the medium was removed and 100 µL DMSO were added to each well. The plates were then shaken thoroughly for some minutes and the absorbance was measured at 570 nm using a iMark micro plate reader (Biorad). Cell viability was reported as percentage of death cells observed in treated samples relative to that observed in not treated control cells. All results were analyzed as the mean ± standard deviation (SD) of the mean values. The EC50 values of each compound were calculated by fitting the Dose Response MTT curve with a Origin8 software using the equation: y=A1 + (A2-A1)/(1+10^((LOGx0-x)*p)) where A1 and A2 are bottom and top asymptote, respectively; LOGx0 and p are center and hill slope, respectively.

2.6 Apoptosis analysis

Apoptosis was detected using an Annexin V et Dead Cell Detection Kit (Millipore) and determined by the Muse™ Cell Analyzer. MCF7 cells were seeded in a 12-well plate (6×10^4 cells/well) and incubated with Cur-HoS-Apo (2.74 µM Cur), Que-HoS-Apo (3 µM Que), Que-Cur-HoS-Apo (2.74 µM Cur + 3 µM Que) for 48 h at 37°C. The cells were detached using trypsin/EDTA (Ethylenediaminetetraacetic acid) and washed with PBS. The cells were resuspended in 80 µL cell culture medium and 80 µL Annexin kit solution and incubated at

room temperature in the dark for 30 min. The samples were immediately analyzed by the Muse™ Cell Analyzer. The results were obtained by three independent experiments.

2.7 Measurement of intracellular reactive oxygen species (ROS)

To evaluate the effect of the compounds on ROS generation, MCF7 cells were seeded in a 12-well plate (6×10^4 cells/well) and incubated with the different compounds combination at the same concentrations used for the apoptosis detection protocol. After 48 h of exposure at 37°C, according to the manufacturer's protocol, cells were detached, resuspended at 1×10^6 cells/mL and incubated at 37°C for 30 min with Muse™ Oxidative Stress working solution. The number of ROS positive cells were assessed using the Muse™ Cell Analyzer. The results were obtained by three independent experiments.

2.8 Cellular uptake studies

To follow the internalization of the different compounds into MCF7 cells, the fluorescence intensity of Curcumin was measured by means of confocal microscope. Hence, MCF7 cells were seeded on µ-slide 8 well (Chambered Coverslip for Cell Imaging - ibidi) and incubated overnight. Subsequently, cells were treated with Que-Cur-HoS-Apo at a dose of 2.74 µM Cur + 3 µM Que and the free combination (Que + Cur) for 48 h at 37°C. Finally, cells were washed twice with PBS and stained with DiD (Vybrant® Dil Cell-Labeling Solution) according to the manufacturer's instructions to visualize the cell membrane and cell integrity. Samples were analyzed under a confocal microscope Leica TCS SP8 with the filter of 405-nm excitation and 488-nm emission wavelengths.

3. Results

3.1 Nanoparticle characterization

In this study, the encapsulation of both Quercetin (Que) and Curcumin (Cur) into HoS-Apo cavity was carried out by disassemble and reassemble of HoS-Apo cage at pH 2 and 7.4, respectively, after the addition of natural compounds (Figure 1)[24]. The number of molecules that remained entrapped in the Apoferritin after the dissociation/reassociation procedure was detected by HPLC using a reverse phase column and are reported in Table 1.
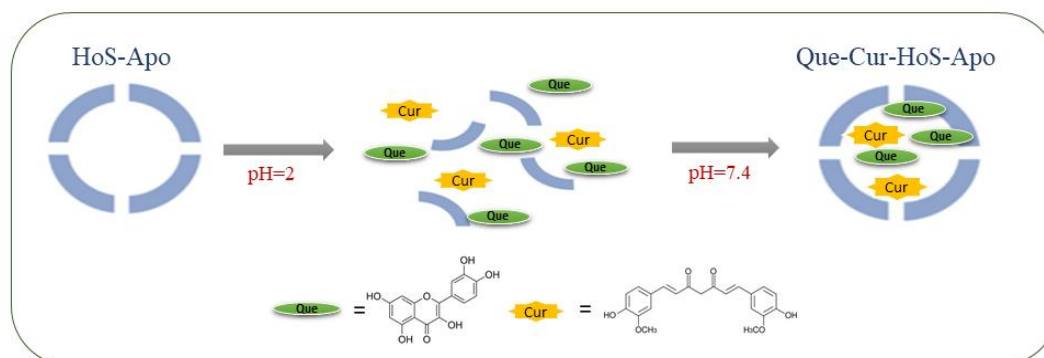
Figure 1. Schematic representation of the Quercetin and Curcumin loading process into the internal apoferritin cavity.

Cur showed a three times higher encapsulation efficiency then Que when loaded separately (1:200±20 and 1:74±9 for Cur and Que, respectively) in Apoferritin. Whereas when loaded together, Que and Cur showed a similar loading of 82±2 and 73±7, respectively. The encapsulation of the compounds in the protein cage was followed by size exclusion chromatography by comparing the curves acquired at 280 nm, 370 nm and 430 nm, corresponding to the maximum absorbance of the protein, Que and Cur, respectively. Fig. 2A and 2B show that the chromatographic peak obtained at 370 nm (pink curve) and 430 nm (red curve) of the Que or Que+Cur loaded into HoS-Apo (namely, Que-HoS-Apo and Que-Cur-HoS-Apo, respectively) had the same retention time of native HoS-Apo (blue curve, 280 nm). These results demonstrate unequivocally the co-localization of Quercetin, Curcumin and the protein. The gel filtration chromatogram obtained (Figure 2C) without disassembling the protein at pH 2 showed the absence of peaks (370 nm, 430 nm) with the same retention time of HoS-Apo. These observations allow to confirm the efficacy of washing steps by dialysis to eliminate Que and Cur non-specifically bound to the external surface of the protein. The hydrated mean diameter of native HoS-Apo, Que-HoS-Apo, Que-HoS-Apo and Que-Cur-HoS-Apo was determined using DLS. The average particle size of Cur-HoS-Apo, Que-HoS-Apo and Que-Cur-HoS-Apo nanoparticles were 17.7±2.2 nm, 15.8±1.9 nm and 17.4±1.2, respectively (Figure S1, supplementary materials). These values are slightly higher than native HoS-Apo size, 12.9±1 nm.
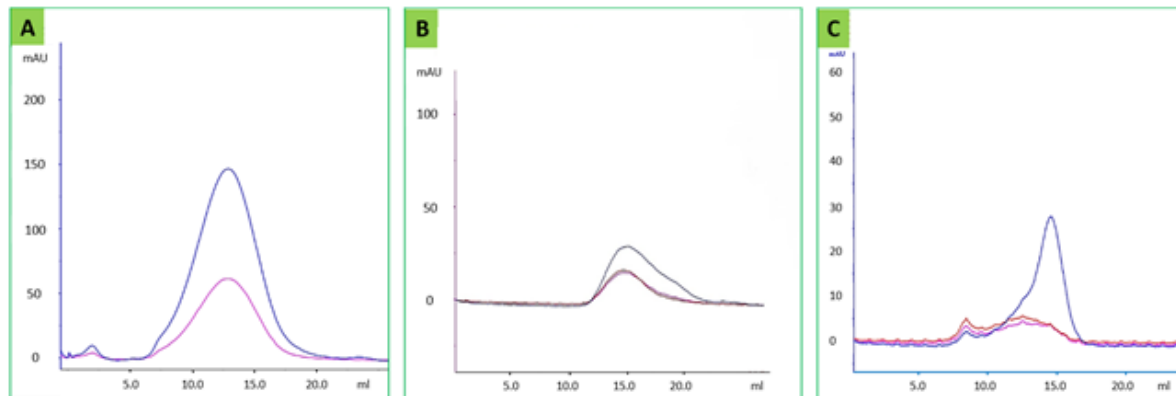

Figure 2. Size exclusion chromatograms. (A) Quercetin (pink curve) and HoS-Apo (blue curve) chromatograms obtained after dissociation/reassociation procedure. (B) Quercetin (pink curve), Curcumin (red curve) and HoS-Apo (blue curve). (C) Chromatograms obtained after incubation of the Quercetin and Curcumin with HoS-Apo at pH 7.4 without dissociation/reassociation procedure.

The release of Que and Cur from HoS-Apo was assessed at 37 °C under dialysis at different time intervals, by measuring the concentrations by HPLC. It appears evident that Que is released faster than Cur. As it has been showed below, the fast release of Que, do not decrease

the toxic effect of this natural compound that is further increased once administered loaded in the protein cavity (Figure 3).
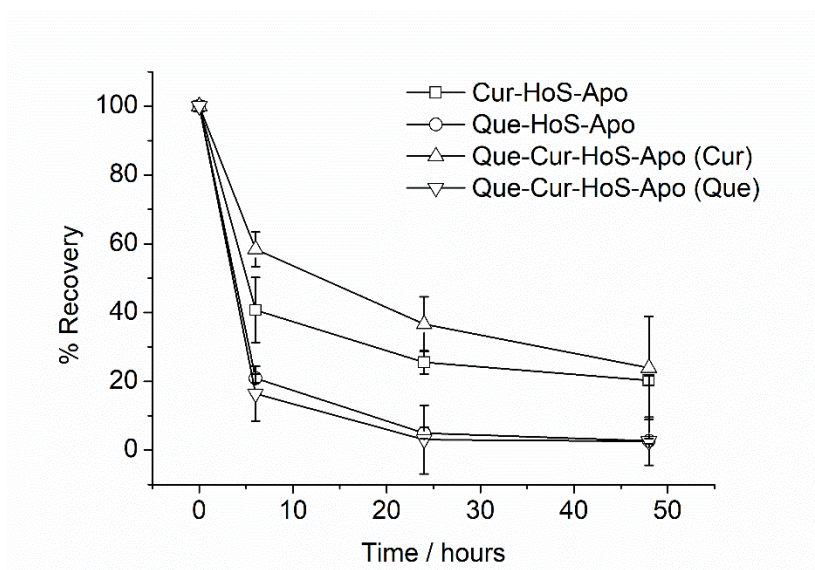

Figure 3: In vitro stability of Que and Cur loaded in HoS-Apo evaluated at different times (6, 24 and 48h) under dialysis in NaCl HEPES buffer at 37°C, pH = 7.4. Graph shows the mean ±SD of % Que and Cur obtained by 3 independent experiments.

3.2 *In vitro* cytotoxicity

Viability of human breast cancer cells (MCF7) was determined by MTT assay after exposure to various concentrations of free Que and Cur and their HoS-Apo derivatives. Firstly, Quercetin and Curcumin cytotoxicity was analyzed. Cells were treated with different concentrations of Que and Cur for 48 h (Figure 4A). The graph shows a detectable toxicity in a dose dependent manner for both anti-cancer agents. Moreover, Figure 4B shows that Que and Cur incubated alone or in combination exhibited a significantly lower cytotoxic effect compared to the Apoferritin encapsulated forms. In order to assess the toxic effect of the compounds on normal cells, the MTT assay was carried out with the non-tumorigenic breast epithelial cell line MCF10A (Figure 4C-D). Interestingly, the compounds exhibit a low cytotoxicity compared to MCF7 cells when they are administered encapsulated alone or co-encapsulated in the protein cavity (Figure 4D). On the contrary, when Que and Cur are incubated in free combination, display a higher cytotoxicity similar in the two cell lines under consideration (Figure 4A-C). Moreover, unloaded Apoferritin administered alone was not toxic in the range of concentrations used (Figure 4B-D).
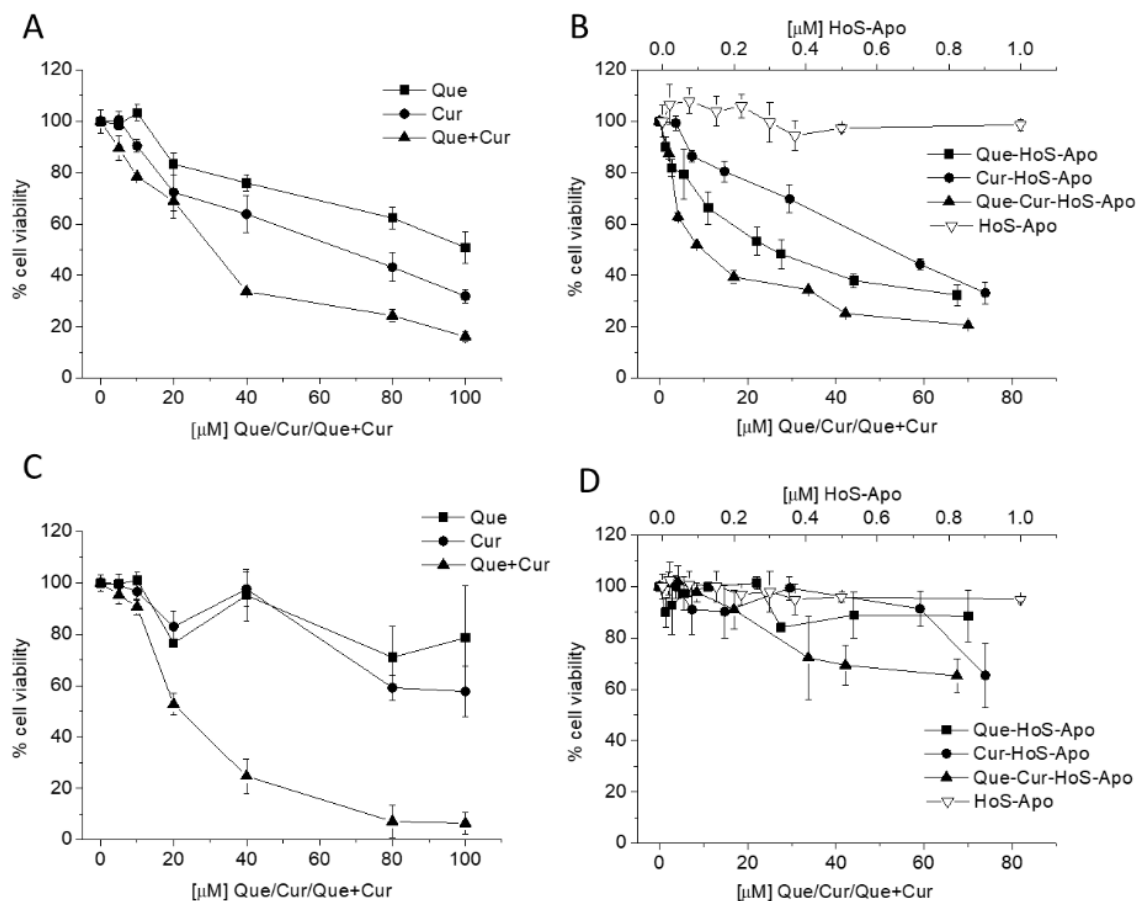
Figure 4. Percentage of viability (measured with MTT assay) of MCF7 breast cancer cells (A, B) and MCF10A non-tumorigenic breast epithelial cells (C, D) after 48 h of incubation with different concentrations of Que, Cur, Que + Cur (A, C) or Que-HoS-Apo, Cur-HoS-Apo, Que-Cur-HoS-Apo and HoS-Apo (B, D), respectively. Graphs show the mean ± SD of percentage viability evaluated on three independent experiments.

In MCF7 the EC50 (half maximal effective concentration) of Que and Cur measured when the compounds were administered alone, reported in Table 2, is higher (58.5 and >100 µM) than the EC50 obtained after their encapsulation in the Apoferritin cavity. Interestingly, with Que-Cur-HoS-Apo formulation a marked reduction of EC50 (11 µM) was observed. This value is significantly lower with respect to the EC50 calculated when the compounds were administered in free combination (28.6 µM). On the contrary in MCF10A only in the case of Que and Cur incubated in free combination, the EC50 was similar to MCF7 (20.8 µM), while in any other formulation of Que and Cur is > 100 µM.

3.3 Apoptosis analysis by Annexin-V/ 7-Amino-Actinomycin (7-AAD) Staining Assay

Apoptosis was detected using an Annexin detection kit. The number of cells undergoing early apoptosis (positive for Annexin V and negative for 7-AAD) and late apoptosis (double-positive for Annexin V and 7-AAD) was quantified using flow-cytometry (by Muse instrument). As shown in Figure 5, the percentage of cells in early apoptosis and of late apoptotic/dead cells

increased only after Que-Cur-HoS-Apo treatment compared to Que and Cur HoS-Apo. From these results, it is possible to conclude that Que-Cur-HoS-Apo treatment could cause late-stage apoptosis and cell death.
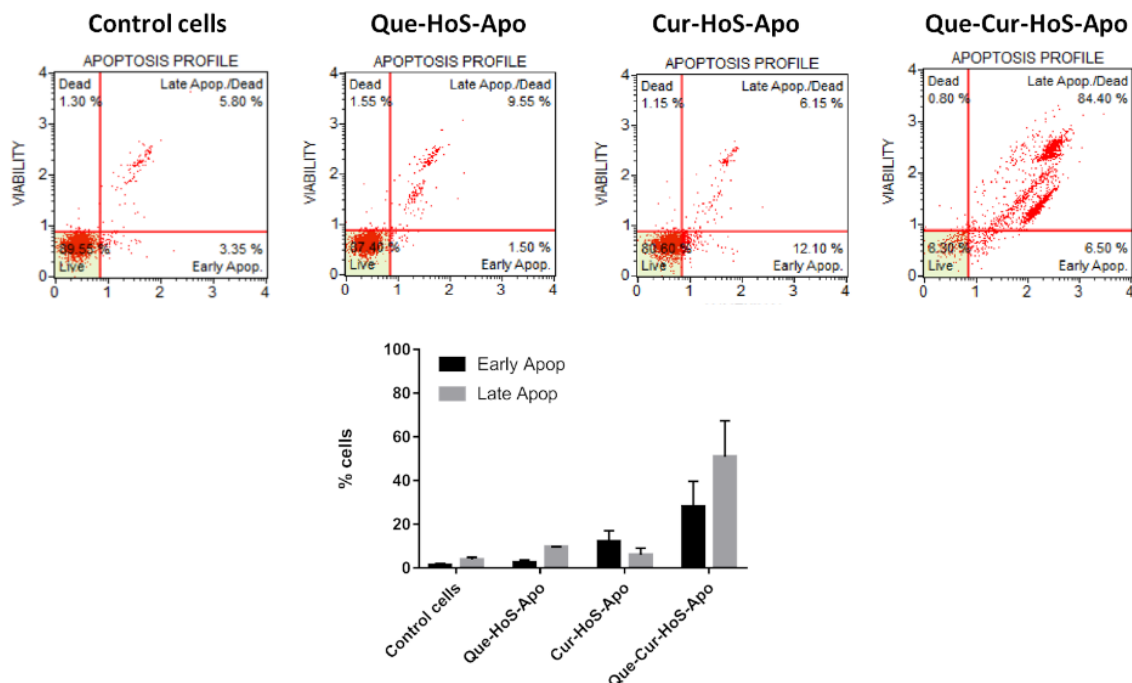

Figure 5. Flow cytometry analysis of MCF7 cells positive for Annexin-V after treatment with Que-HoS-Apo, Cur-HoS-Apo and Que-Cur-HoS-Apo for 48 h. Representative plots are shown in the figure. The graph shows the percentage of early apoptotic (positive for Annexin V and negative for 7-AAD) and late apoptotic cells (positive for both Annexin V and 7-AAD). Results are expressed as mean ± SEM of three independent experiments.

3.4 Measurement of intracellular reactive oxygen species (ROS)

Intracellular ROS levels were measured by using Oxidative Stress Kit (Figure 6). In the ROS histogram, M1 and M2 represent different cellular populations according to levels of intracellular ROS: the blue area (M1) corresponds to cells negative for ROS production and the red area (M2) to cells positive for ROS production. The combination of Que and Cur in HoS-Apo showed a significant increase of the ROS levels in MCF7 cells with almost 75% of the ROS (+) cells in comparison to the control cells after 48 h of incubation. Moreover, ROS level were particularly higher also for the Cur-HoS-Apo and lower for Que-HoS-Apo.
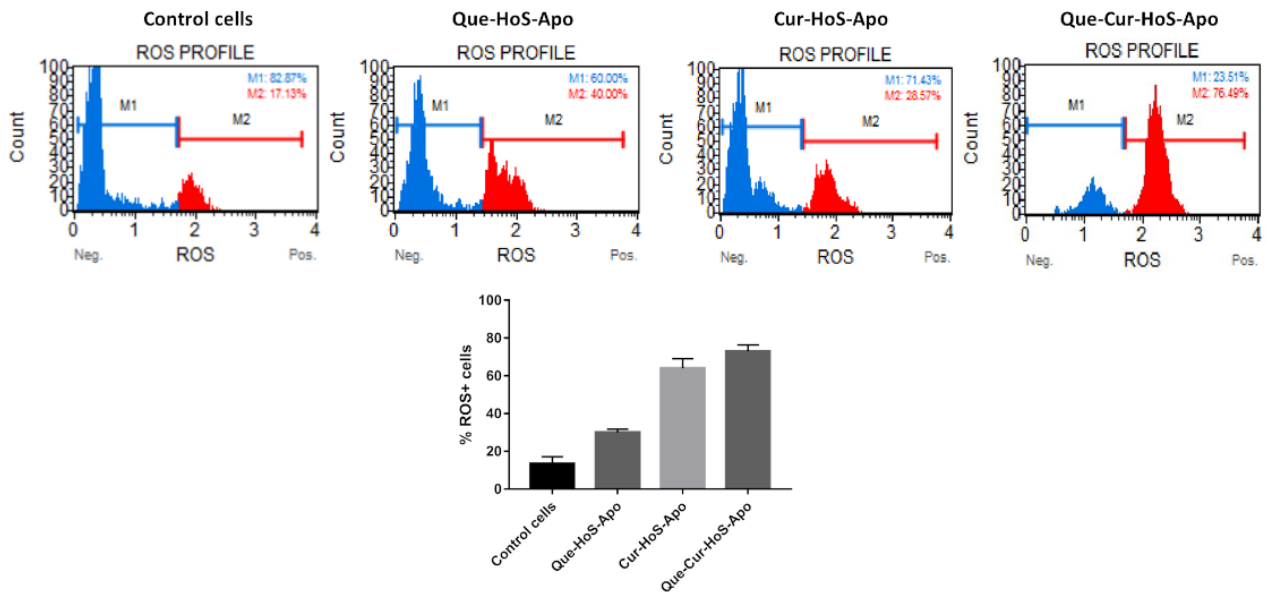
Figure 6: Detection of ROS production by MCF7 cells after treatment with Que-HoS-Apo, Cur-HoS-Apo and Que-Cur-HoS-Apo for 48 h. Representative plots are shown in the figure. Graph shows the percentage of ROS positive cells in basal condition and after treatment. Results are expressed as mean ± SEM of three independent experiments.

3.5 Cellular uptake studies by immunohistochemistry

The intracellular uptake was analyzed by fluorescence microscopy imaging, as shown in Figure 7. Red fluorescence represents DiD and green fluorescence represents Cur. Green Cur fluorescence was detected in the cells treated for 48 h with free Que + Cur. On the contrary, cells treated with Que-Cur-HoS-Apo emitted a strong fluorescence in the cytoplasm of MCF7 cells, that was attributed to Cur, indicating that Que-Cur-HoS-Apo nanoparticles entered more efficiently the cells with respect to the free compounds.
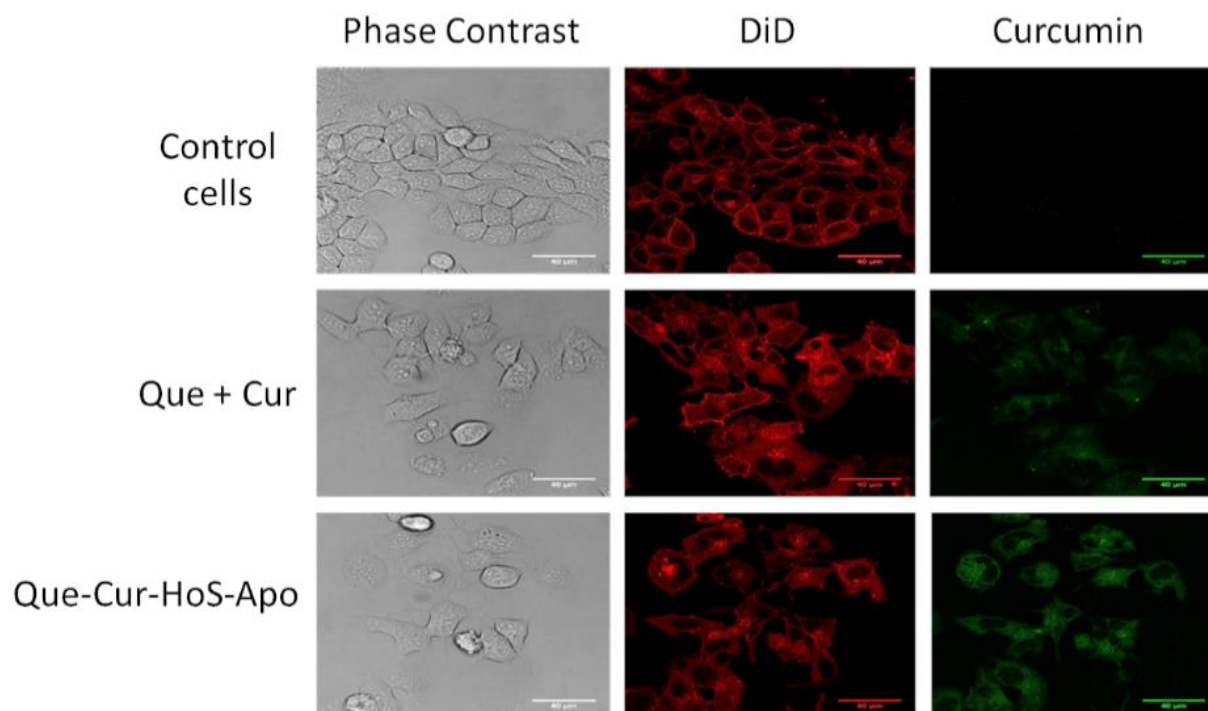
Figure 7. In vitro evaluation by means of confocal microscopy of Que + Cur and Que-Cur-HoS-Apo uptake by MCF7 upon 48 h of incubation. MCF7 cells were stained with DiD in order to visualize the plasma membrane. The natural fluorescence signal of Curcumin was exploited as an indicator of the presence of protein nanoparticles in the cytoplasm. Scale bars = 40µm.

4. Discussion

Combinations of natural compounds have been investigated in the treatment of different types of cancer to obtain a more efficient therapeutic effect with lower dosage and to reduce drug resistance and side effects[28]. In a research by Mertens-Talcott *et al.*[29], it was shown that Quercetin and Ellagic acid can synergistically reduce proliferation and viability of the MOLT-4 human leukemia cell line at 5 and 10 µmol/L concentrations. In another study, the combination of Quercetin and Resveratrol showed synergistic effects in HT-29 colon cancer cells[30]. Moreover, a research group reported that Resveratrol and Curcumin are more effective in inhibiting the growth of human colon cancer HCT-116 cells[31]. Moreover, Arzuman *et al.* suggested that administration of the platinum-containing pyridine-based ligands acts synergistically in combination with Curcumin and Quercetin against ovarian cancer. [32] In another studiy, chemopreventive efficacies of Curcumin and Quercetin via induction of apoptosis were assessed during BP-induced lung carcinogenesis[33].

Quercetin and Curcumin are renowned phytochemicals which possess specific chemical structures and exhibit significant anti-cancer activities exploiting different molecular mechanisms. Zang *et al.* and Mutlu Altundağ *et al.* reported that the combination treatment of both Quercetin and Curcumin could employ different signaling pathways simultaneously and therefore exert synergistic cancer chemopreventive effects[18, 34]. Moreover, few studies have been carried out on the evaluation of the efficacy of different polyphenolic compounds after

13

their encapsulation into nanoparticles. The present study provides novel targeted nanoparticles of natural origin to further enhance the combined effect of Que and Cur.

In this study, Cur or Que incubated alone showed, on MCF7 cells, an EC50 of *ca.* 50 μM and > 100 μM, respectively, both consistent with results already reported in literature[27, 35, 36]. The encapsulation inside the Apoferritin cavity reduced significantly the EC50 to 24 and 47.5 μM for Que-HoS-Apo and Cur-HoS-Apo, respectively. This is probably due to the enhanced uptake caused by the Apoferritin delivery. On the contrary, Que and Cur incubated in combination are taken up aspecifically and they display an enhanced cytotoxicity on both MCF7 and MCF10A cells. On the contrary, the MTT curve analysis indicates that Que-Cur-HoS-Apo markedly exerted synergistic growth inhibitory effects on MCF-7 with respect to MCF10. In fact, the EC50 for MCF7 resulted further reduced to 11 μM whereas for MCF10 it remains > 100 μM. The results of Annexin-V/7-AAD staining assay (Figure 5) were consistent with the MTT results.

The design of suitable molecular carriers for natural compounds has provided unprecedented opportunities to increase significantly their stability, solubility, bioavailability and targeting capabilities. As shown by Prosad *et al.* and Srinivas *et al.*, Quercetin solubility in aqueous solution ranges from 0.00215 g/L at 25°C to 0.665 g/L at 140°C and Curcumin solubility in aqueous solution is 0.6 μg/mL [37, 38]. So far, the poor pharmacodynamics of natural compounds was one of the reason that has hampered translation into clinics. The way to overcome this limitation could be to design nanosized systems able to encapsulate bioactive compounds in order to favour their bio-availability[27]. Our results showed that the encapsulation into Apoferritin of Que and Cur produced synergistically greater inhibition of MCF7 viability than the administration of the same dose as free combination. One can surmise that the use of the same nanocarrier for both bioactive compounds improve their therapeutic effect on cells due to their simultaneous delivery in the same cell compartment. About this, it was previously reported by our group that MCF7 cells express a high concentration of scavenger receptors class A member 5 (SCARA5) on their cytoplasmic membrane, able to internalize L-ferritin[27]. Competition studies demonstrated that, HoS-Apo is taken-up by these cells through SCARA5 by receptor mediated endocytosis. Recently, it has been published by our group that HoS-Ferritin (loaded with iron oxide) is also taken-up by a murine adenocarcinoma cell line (TS/A) both in cell culture and mice model and accumulates into endosomal vesicles[39]. The low pH of these vesicles can trigger the release of the iron payload or bioactive compounds thus inducing the toxic effect at endosomal level. In particular, ROS generation is responsible for the destabilization of endosomal/lysosomal membrane [39].Accordingly, the results reported in this study show that Que-, Cur- and Que-Cur-HoS-Apo increased the levels of ROS upon incubation on MCF7 cells (Figure 5). The same effect was observed using many anti-cancer compounds [40], that cause cancer cell death.

Finally, physicochemical characteristics such as particle size, solubility, surface charge and surface properties would influence cellular internalization[41]. Ferritin shows positive or close to zero charge density on its exterior surface at pH 7.0 thus exhibiting a stronger affinity for the negatively charged cell membrane[42]. In fact, fluorescence microscopy images showed considerable internalization of Que-Cur-HoS-Apo in MCF7 cells compared to Que + Cur

administered alone (Figure 7). Moreover, apoferritin and ferritin particles have a narrow size of about 13 nm. It was found that the internalization of relatively small nanoparticles (< 50 nm) is facilitated than the larger ones[43].

Another important point in this context is the competitive binding of these bioactive compounds to blood proteins that may significantly reduce their delivery to cells and target tissues[44, 45]. It was indicated that, the high affinity of Que for serum albumin caused its slow elimination from the body[46]. Similar results showed that, epigallocatechin-3-O-gallate, presenting an high affinity for blood proteins, could potentially improve its half-life in the body[47]. On these basis, one can surmise that the sequestration of Que and Cur inside the Apoferritin cavity prevents their binding to serum proteins, thus increasing the amount of bioactive compounds available for tumor cell internalization.

5.   Conclusions

In conclusion, the simultaneous loading of Que and Cur into the Apoferritin cavity improves their synergistic cytotoxic effect by enhancing bio-availability and effective targeting of MCF7 human breast cancer cells. Interestingly, the entrapment of Que and Cur into Apoferritin reduce significantly the cytotoxic effect for MCF10A cells that are widely used non-malignant breast epithelial cells The use of an appropriate molar ratio of Que/Cur leads to a considerable reduction of MCF7 cell proliferation and apoptosis at a lower Quercetin and Curcumin concentration than free combination. In

Table 1.

Table 1: Encapsulation efficacy of Quercitin (Que), Curcumin (Cur) and their combination in the Apoferritin protein core. Results are expressed as mean ± SD evaluated on three different experiments.

Sample	Que (μM)	Cur (μM)	HoS-Apo (μM)	HoS-Apo: Que ratio	HoS-Apo: Cur ratio
Que-HoS-Apo	1620±136	---	22±2	1:74±9	---
Cur-HoS-Apo	---	4989±459	25±1.5	---	1:200±20
Que-Cur-HoS-Apo	1715±171	1537±274	21±3	1:82±2	1:73±7

Table 2.

Table 2. The EC50 of Cur, Que, Cur + Que before and after Apoferritin encapsulation towards MCF7 and MCF10A cells.

Cells	Que	Cur	Que+Cur	Que-HoS-Apo	Cur-HoS-Apo	Que-Cur-HoS-Apo
MCF-7	>100 μM	58.5 μM	28.6 μM	24 μM	47.5 μM	11 μM
MCF-10A	> 100 μM	>100 μM	20.8 μM	> 100 μM	> 100 μM	> 100 μM

6.   References

1.   Tao, Z., et al., *Breast cancer: epidemiology and etiology.* Cell biochemistry and biophysics, 2015. **72**(2): p. 333-338.
2.   DeSantis, C.E., et al., *Breast cancer statistics, 2017, racial disparity in mortality by state.* CA: a cancer journal for clinicians, 2017. **67**(6): p. 439-448.
3.   Dominietto, M., N. Tsinoremas, and E. Capobianco, *Integrative analysis of cancer imaging readouts by networks.* Molecular oncology, 2015. **9**(1): p. 1-16.
4.   Senapati, S., et al., *Controlled drug delivery vehicles for cancer treatment and their performance.* Signal transduction and targeted therapy, 2018. **3**(1): p. 7.
5.   Bishayee, A. and G. Sethi. *Bioactive natural products in cancer prevention and therapy: Progress and promise*. in *Seminars in cancer biology*. 2016. Elsevier.
6.   Samarghandian, S. and M.M. Shabestari, *DNA fragmentation and apoptosis induced by safranal in human prostate cancer cell line.* Indian journal of urology: IJU: journal of the Urological Society of India, 2013. **29**(3): p. 177.
7.   Chen, A.Y. and Y.C. Chen, *A review of the dietary flavonoid, kaempferol on human health and cancer chemoprevention.* Food chemistry, 2013. **138**(4): p. 2099-2107.
8.   Gibellini, L., et al., *Quercetin and cancer chemoprevention.* Evidence-based complementary and alternative medicine, 2011. **2011**.
9.   Nam, J.-S., et al., *Application of bioactive quercetin in oncotherapy: from nutrition to nanomedicine.* Molecules, 2016. **21**(1): p. 108.
10.   Filipa Brito, A., et al., *Quercetin in cancer treatment, alone or in combination with conventional therapeutics?* Current medicinal chemistry, 2015. **22**(26): p. 3025-3039.
11.   Duvoix, A., et al., *Chemopreventive and therapeutic effects of curcumin.* Cancer letters, 2005. **223**(2): p. 181-190.
12.   D'Archivio, M., et al., *Bioavailability of the polyphenols: status and controversies.* International journal of molecular sciences, 2010. **11**(4): p. 1321-1342.
13.   Wang, S., et al., Delivering flavonoids into solid tumors using nanotechnologies. Expert opinion on drug delivery, 2013. 10(10): p. 1411-1428.
14.   Fantini, M., et al., *In vitro and in vivo antitumoral effects of combinations of polyphenols, or polyphenols and anticancer drugs: perspectives on cancer treatment.* International journal of molecular sciences, 2015. **16**(5): p. 9236-9282.
15.   Lewandowska, U., et al., *Synergistic interactions between anticancer chemotherapeutics and phenolic compounds and anticancer synergy between polyphenols.* Advances in Hygiene & Experimental Medicine/Postepy Higieny i Medycyny Doswiadczalnej, 2014. **68**.
16.   Silva, R., et al., *Modulation of P-glycoprotein efflux pump: induction and activation as a therapeutic strategy.* Pharmacology & therapeutics, 2015. **149**: p. 1-123.
17.   Azevedo, M.I., et al., *The antioxidant effects of the flavonoids rutin and quercetin inhibit oxaliplatin-induced chronic painful peripheral neuropathy.* Molecular Pain, 2013. **9**(1): p. 53.
18.   Zhang, J.-Y., et al., *Combinational treatment of curcumin and quercetin against gastric cancer MGC-803 cells in vitro.* Molecules, 2015. **20**(6): p. 11524-11534.
19.   Watkins, R., et al., *Natural product-based nanomedicine: recent advances and issues.* International journal of nanomedicine, 2015. **10**: p. 6055.
20.   Shi, J., et al., *Cancer nanomedicine: progress, challenges and opportunities.* Nature Reviews Cancer, 2017. **17**(1): p. 20.
21.   Cutrin, J.C., et al., *Curcumin/Gd loaded apoferritin: a novel "theranostic" agent to prevent hepatocellular damage in toxic induced acute hepatitis.* Molecular pharmaceutics, 2013. **10**(5): p. 2079-2085.
22.   Petruk, G., et al., *Encapsulation of the Dinuclear Trithiolato-Bridged Arene Ruthenium Complex Diruthenium-1 in an Apoferritin Nanocage: Structure and Cytotoxicity.* ChemMedChem, 2019. **14**(5): p. 594-602.

23.   Truffi, M., et al., *Ferritin nanocages: A biological platform for drug delivery, imaging and theranostics in cancer.* Pharmacological research, 2016. **107**: p. 57-65.

24.   Conti, L., et al., *L-Ferritin targets breast cancer stem cells and delivers therapeutic and imaging agents.* Oncotarget, 2016. **7**(41): p. 66713.

25.   Turino, L.N., et al., *Ferritin decorated PLGA/paclitaxel loaded nanoparticles endowed with an enhanced toxicity toward MCF-7 breast tumor cells.* Bioconjugate chemistry, 2017. **28**(4): p. 1283-1290.

26.   Monti, D., G. Ferraro, and A. Merlino, *Ferritin-based anticancer metallodrug delivery: Crystallographic, analytical and cytotoxicity studies.* Nanomedicine: Nanotechnology, Biology and Medicine, 2019.

27.   Geninatti Crich, S, et al., *Targeting ferritin receptors for the selective delivery of imaging and therapeutic agents to breast cancer cells.* Nanoscale, 2015. **7**(15): p. 6527-6533.

28.   Nobili, S., et al., *Natural compounds for cancer treatment and prevention.* Pharmacological research, 2009. **59**(6): p. 365-378.

29.   Mertens-Talcott, S.U., S.T. Talcott, and S.S. Percival, *Low Concentrations of Quercetin and Ellagic Acid Synergistically Influence Proliferation, Cytotoxicity and Apoptosis in MOLT-4 Human Leukemia Cells–.* The Journal of nutrition, 2003. **133**(8): p. 2669-2674.

30.   Del Follo-Martinez, A., et al., *Resveratrol and quercetin in combination have anticancer activity in colon cancer cells and repress oncogenic microRNA-27a.* Nutrition and cancer, 2013. **65**(3): p. 494-504.

31.   Majumdar, A.P., et al., *Curcumin synergizes with resveratrol to inhibit colon cancer.* Nutrition and cancer, 2009. **61**(4): p. 544-553.

32.   Arzuman, L., Beale, P., Yu, J.Q., Huq, F. *Monofunctional Platinum-containing Pyridine-based Ligand Acts Synergistically in Combination with the Phytochemicals Curcumin and Quercetin in Human Ovarian Tumour Models.* Anticancer Res. 2015. **35**(5):2783-94.

33.   Liu, Y., Wu, Y.M., Zhang, P.Y., *Protective effects of curcumin and quercetin during benzo(a)pyrene induced lung carcinogenesis in mice.* Eur Rev Med Pharmacol Sci. 2015;**19**(9):1736-43.

34.   Mutlu Altundağ, E., et al., *Synergistic Induction of Apoptosis by Quercetin and Curcumin in Chronic Myeloid Leukemia (K562) Cells.* Nutrition and cancer, 2018. **70**(1): p. 97-108.

35.   Hashemzaei, M., et al, *Anticancer and apoptosis inducing effects of quercetin in vitro and in vivo.* Oncol Rep. 2017 ;**38**(2):819-8.

36.   Khorsandi, L., Orazizadeh, M., Niazvand, F., Abbaspour, M.R., Mansouri, E., Khodadadi, A. *Quercetin induces apoptosis and necroptosis in MCF-7 breast cancer cells.* Bratisl Lek Listy. 2017;118(2):123-128.

37.   Prasad, S., A.K. Tyagi, and B.B. Aggarwal, *Recent developments in delivery, bioavailability, absorption and metabolism of curcumin: the golden pigment from golden spice.* Cancer research and treatment: official journal of Korean Cancer Association, 2014. **46**(1): p. 2.

38.   Srinivas, K., et al., *Solubility and solution thermodynamic properties of quercetin and quercetin dihydrate in subcritical water.* Journal of Food Engineering, 2010. **100**(2): p. 208-218.

39.   Bitonto V, Alberti D, Ruiu R, Aime S, Geninatti Crich S, Cutrin JC. L-ferritin: *A theranostic agent of natural origin for MRI visualization and treatment of breast cancer.* J Control Release. 2019 Dec 31. pii: S0168-3659(19)30770-9. doi: 10.1016/j.jconrel.2019.12.051.

40.   Li, W., et al., *Combination of quercetin and hyperoside has anticancer effects on renal cancer cells through inhibition of oncogenic microRNA-27a.* Oncology reports, 2014. **31**(1): p. 117-124.

41.   He, C., et al., *Effects of particle size and surface charge on cellular uptake and biodistribution of polymeric nanoparticles.* Biomaterials, 2010. **31**(13): p. 3657-3666.

42.   Zang, J., et al., *Ferritin cage for encapsulation and delivery of bioactive nutrients: From structure, property to applications.* Critical reviews in food science and nutrition, 2017. **57**(17): p. 3673-3683.

43.   Donkor, D.A. and X.S. Tang, *Tube length and cell type-dependent cellular responses to ultra-short single-walled carbon nanotube.* Biomaterials, 2014. **35**(9): p. 3121-3131.

44.   Salatin, S., S. Maleki Dizaj, and A. Yari Khosroushahi, *Effect of the surface modification, size, and shape on cellular uptake of nanoparticles.* Cell biology international, 2015. **39**(8): p. 881-890.

45.   Jakobek, L., *Interactions of polyphenols with carbohydrates, lipids and proteins.* Food Chemistry, 2015. **175**: p. 556-567.

46.   Manach, C., et al., *Quercetin metabolites in plasma of rats fed diets containing rutin or quercetin.* The Journal of nutrition, 1995. **125**(7): p. 1911-1922.

47.   Eaton, J.D. and M.P. Williamson, *Multi-site binding of epigallocatechin gallate to human serum albumin measured by NMR and isothermal calorimetry.* Bioscience reports, 2017: p. BSR20170209.